

COMPARISON OF PRONY AND EIGENANALYSIS FOR POWER SYSTEM CONTROL DESIGN

C.E. Grund J.J. Paserba
Senior Member, IEEE Member, IEEE

GE Industrial and Power Systems
Power Systems Engineering Department
Schenectady, New York

J.F. Hauer
Fellow, IEEE
Bonneville Power Administration
Portland, Oregon

S. Nilsson
Fellow, IEEE
EPRI
Palo Alto, California

Abstract - This paper describes comparative results of direct (eigenanalysis) and indirect (Prony analysis) methods for generating frequency-domain data for power system control design. The methods are applied to the same model, a medium-scale model of the Midcontinent Area Power Pool (MAPP). Modal parameters (frequencies and damping) and transfer function poles and zeros are compared as calculated by the two methods.

Key Words - Power System Analysis, Frequency Domain Analysis [2], Control Design, Prony Analysis [4], Eigenanalysis.

INTRODUCTION

Frequency domain analysis for control systems and mechanical vibration analysis has been the norm for decades. In the power system area these techniques have also been applied to small systems such as single machines with excitation and other controls. However, applications to large power systems have more recently resulted in the development of advanced and robust numerical techniques in the derivation of state variable models and eigenanalysis of these models [3, 14].

The derivation of low-order control design models from standard stability models can take several paths. One methodology involves dynamic equivalencing, eigenanalysis and pole/zero cancellation [1]. In this method transfer functions were derived using eigenanalysis of a medium-scale model. FFT analysis of the large-scale stability model was used for validation. A second option is the use of Prony analysis of large-scale model time-domain simulations. The latter method appears to have several advantages over eigenanalysis. The most important one is that it does not require the derivation of a medium-scale model. Also, system-wide changes can only be modeled by a large-scale model and therefore a new medium-scale model would have to be derived. Additionally, Prony analysis can also be applied to field measurements for the derivation of control design models.

Previous validation [3] was performed on analytic functions and on power system field test responses. Sliding window analysis and analysis of responses at widely separated locations identified the dominant electromechanical modes consistently. However independent validation was not performed on the field measurements. The above reasons bring out the importance of additional analytical validation of the Prony method.

This paper presents summary discussions and comparative results and analysis of the two methods. The two methods are described briefly and important input data constants are discussed. They are applied to a medium-scale stability studies data set and the results are compared. The methods are applied to determine modal parameters (modal frequencies and their corresponding damping) and the poles and zeros of transfer functions.

92 SM 541-3 PWRs A paper recommended and approved by the IEEE Power System Engineering Committee of the IEEE Power Engineering Society for presentation at the IEEE/PES 1992 Summer Meeting, Seattle, WA, July 12-16, 1992. Manuscript submitted December 5, 1991; made available for printing May 13, 1992.

DESCRIPTION OF THE METHODS OF ANALYSIS

Each method has its own advantages and disadvantages. Some of the important considerations are inclusion of nonlinearities, the size of the model that can be analyzed, the difficulty in the selection of suitable processing parameters, and the reliability of the results. Linearization, of course, eliminates the effects of nonlinearities and, as such, is valid only for small perturbations from the equilibrium. On the other hand, the Prony methodology is applied to nonlinear system simulation results and therefore includes the effects of nonlinearities for the specific perturbation from equilibrium. Therefore, the effects of nonlinearities are represented, but will be perturbation dependent. In full-state eigenvalue analysis, the size of the model is limited to approximately 500 states. This means that a typical stability data set with 2000 buses and 300 machines must be reduced using dynamic equivalencing to about 30 machines and other dynamic devices such as HVDC lines and SVC. For the Prony method, the size of the model is not limited because only the output is analyzed. This means that standard stability study (time-domain) results are directly usable. This eliminates the task of deriving a medium-scale model (500 states) that is required for the linearization method.

The selection of processing parameters is dependent on the robustness of the numerical algorithms. For most complex algorithms, sensitivity should be determined for each power system model to be analyzed. Additionally, complex numerical algorithms should be validated by an independent methodology as reported in this paper. Prony and eigenanalysis are validated here which also establishes suitable processing parameters for the two methods. Based on the numerical results documented in this paper, the results of the Prony method appear to be more sensitive to changes of the processing parameters. The reliability of results are directly related to algorithm robustness. Many times algorithm robustness is assumed but not tested, resulting in lack of reliability.

Eigenanalysis

Description - This technique calculates state matrices based on sequential state perturbations [2]. Columns of the state (A) and output (C) matrices are calculated based on state perturbations and the input (B) and throughput (D) matrices based on input perturbations, i.e.,

$$\begin{aligned} \Delta \dot{x}_1 / \Delta x_1 &= a_{11} \\ \Delta \dot{x}_2 / \Delta x_1 &= a_{21} \quad \text{etc.} \\ \Delta y_1 / \Delta x_1 &= c_{11} \\ \Delta y_2 / \Delta x_1 &= c_{21} \quad \text{etc.} \end{aligned}$$

Discrete nonlinearities must be linearized using describing functions to be represented properly. This, of course, implies that the results of this type of nonlinearity will be input amplitude dependent. For continuous nonlinearities, a sufficiently small perturbation should be used. Yet the perturbations should be large enough so that their effects influence the interconnected dynamic systems. Positive and negative perturbations are used to increase the accuracy of the linear approximation by averaging. This technique is relatively straightforward to implement on simulation

programs with explicit integration techniques, especially where all differential equations are solved in special subroutines.

The linearization is part of the time-domain simulation software because the effects of each state perturbation must be simulated. Since a network solution is required, its iteration cut-off tolerance must be specified (i.e., per unit active and reactive power mismatch).

State matrices may be used to generate eigenvalues, transfer function zeros, and mode shapes. Additionally, other software may be used to design controllers using output feedback with or without dynamic compensation.

Parameters - Using the state variable perturbation method permits a completely general solution (without analytic linearization) which requires simulation network solutions without advancing time. The network solution cut-off tolerance should be one or more orders of magnitude tighter than for simulations. This is in part due to the small perturbation magnitude (small-signal disturbance). The perturbation amplitude is response amplitude dependent, i.e., it should be large enough to avoid round-off errors and small enough to minimize effects of nonlinearities. The perturbation amplitude also depends on the equilibrium magnitude of the state variable. Smaller amplitude states require smaller perturbations. The state variable amplitudes are perunitized based on rated operating conditions. Perturbations of 1% are normally useful. Non-equilibrium system operating conditions may be used numerically for building state matrices. However, analytically, the resulting matrices do not describe the system modal response, because deviations from non-zero initial conditions are used.

Prony Analysis

Description - This method decomposes time-domain signals into damped sinusoids with four parameters per mode: frequency, damping, amplitude and phase [3,4,5].

$$y(t) = \sum_{i=1}^Q A_i \exp(\sigma_i t) \cos(\omega_i t + \phi_i) \quad (1)$$

Without a detailed derivation, the highlights of the method are:

1. Construct a linear prediction model (Equation (3)) that fits the model (discrete time response at a fixed time interval Δt).
2. Find the roots (eigenvalues) of the linear prediction model.

$$\lambda_{ij} = \sigma_i \pm j\omega_i \quad (2)$$

3. Determine the amplitude and phase of each mode determined in Step 2.

A linear prediction model is given by .

$$y(n) = a_1 y(n-1) + \dots + a_n y(0) \quad (3)$$

i.e., y at t_n is a linear combination of all previous values of y .

Parameters - The most important parameters are the number of data points (N) and the order of the linear prediction model (n), where $n_{\max} = N/2$. The data record length should contain at least two cycles of the known lowest frequency mode. The sample points must be equally spaced and N and n are increased until the signal-to-noise-ratio (SNR) approaches 40 db. The SNR is defined as

$$SNR = 20 \log_{10} \text{rms} [y_i(k)/(y_i(k)-y(k))]$$

where rms indicates the root-mean-square (rms) value, i.e., the square root of the average of the sum of the squares and y is the model and y_i is the input signal.

Lower values of SNR may result in Prony solution errors and usually imply that the linear prediction model order is too low. The full order of the simulation does not determine the linear prediction model order, contrary to conventional wisdom. The controllability of the system for the given input disturbance and the observability of modes in the system output determine the number of modes to be identified, which is usually much lower than the full order of the system [1]. However, the linear prediction model order must be higher than the order determined by controllability/observability because accessory modes are necessary to increase the SNR. Accessory (extraneous) modes fit the inherent noise in the signal, i.e., any deviations from a linear time-invariant system.

Another test on the robustness of the Prony Solution is sliding window fits on the simulation response [3]. The time window is always delayed until after the removal of the system disturbance. Further delays should produce identical Prony Solution assuming the modal response has not decayed yet. In practice, some deviations of the eigenvalues are acceptable. One cause for eigenvalue variations is system nonlinearities with responses dependent on disturbance amplitude.

COMPARISON OF PRONY RESULTS WITH EIGENANALYSIS

In the design of the modal damping controllers (MDC) [6,7] there are two important applications of Prony analysis. It can be used to evaluate the effectiveness of MDC without the system size limitations of eigenanalysis by calculating modal damping with and without MDC using time-domain results. It can also be used to calculate the poles and zeros of control design transfer functions from time-domain results directly. The following is an evaluation of Prony analysis (with comparisons to eigenanalysis results) for these two applications using the same stability data set: Controller performance evaluation and control design model identification.

The test system used for this paper is the Mid-Continent Area Power Pool (MAPP) [7]. The system contains three HVDC systems, one of which is the Square Butte system. It is currently being equipped with an MDCS (Modal Damping Control System) under the EPRI RP1426-4 project. The Square Butte MDCS will use rectifier and inverter ac bus frequencies as input signals and the outputs of the controllers will modulate dc current at the rectifier and dc voltage at the inverters. Therefore, the power system "plant" (i.e., control design model) as seen by the MDCS can be characterized by transfer functions from dc voltage or current to frequency.

The MAPP system is characterized by three major inter-area modes (along with several local modes). These modes are the "MAPP" mode, "Manitoba Hydro" mode (MH), and the "North Dakota" mode (ND). The MAPP mode primarily involves the machines within MAPP swinging against the rest of the eastern USA grid. The MH mode has machines in MAPP swinging against the machines in Manitoba, and the ND mode consists primarily of machines at the Square Butte rectifier end in North Dakota swinging against the machines at the inverter end of the system in Minnesota.

Modal Damping Identification

The test system (450-state MAPP medium-scale model) response for a negative 10% dc voltage pulse is given in Figures 1a and b. Figure 1b shows the 42 MW power pulse. The rectifier and inverter frequency signals used for Prony analysis are given in Figure 1a. The pulse is on from 0.1 to 0.6 s and Prony analysis uses the signals after 0.7 s.

The Prony solution for a relative weight threshold of 0.01 is given in Table 1. Only 20 states (10 modes) are used. Modes 3, 4 and 7 are the MAPP, MH and ND modes. The Prony and input responses match each other with a Signal-to-Noise-Ratio (SNR) of 49 db. The relative weight (amplitude) and phase give modal participation in the input signal. The MAPP mode is dominant, with high relative weight and low damping. The ND mode also has low damping and is evident in the input signal. Other modes with high relative weight have higher damping, i.e., the MH mode. A high

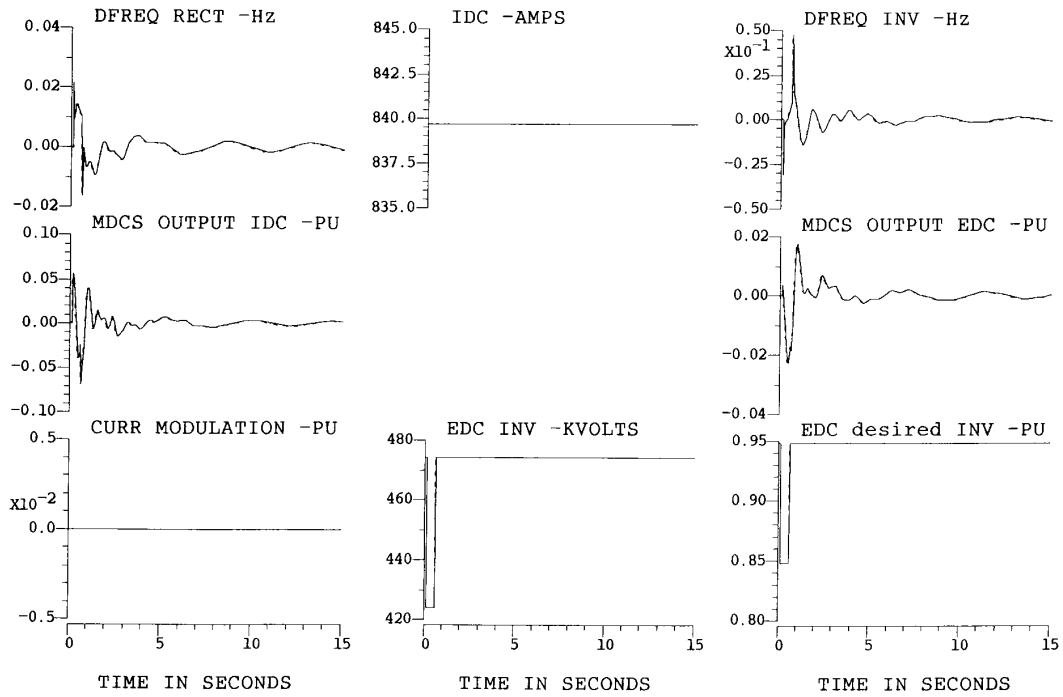


Figure 1a. Medium-scale MAPP model response for Square Butte dc voltage pulse. Square Butte modulation signals.

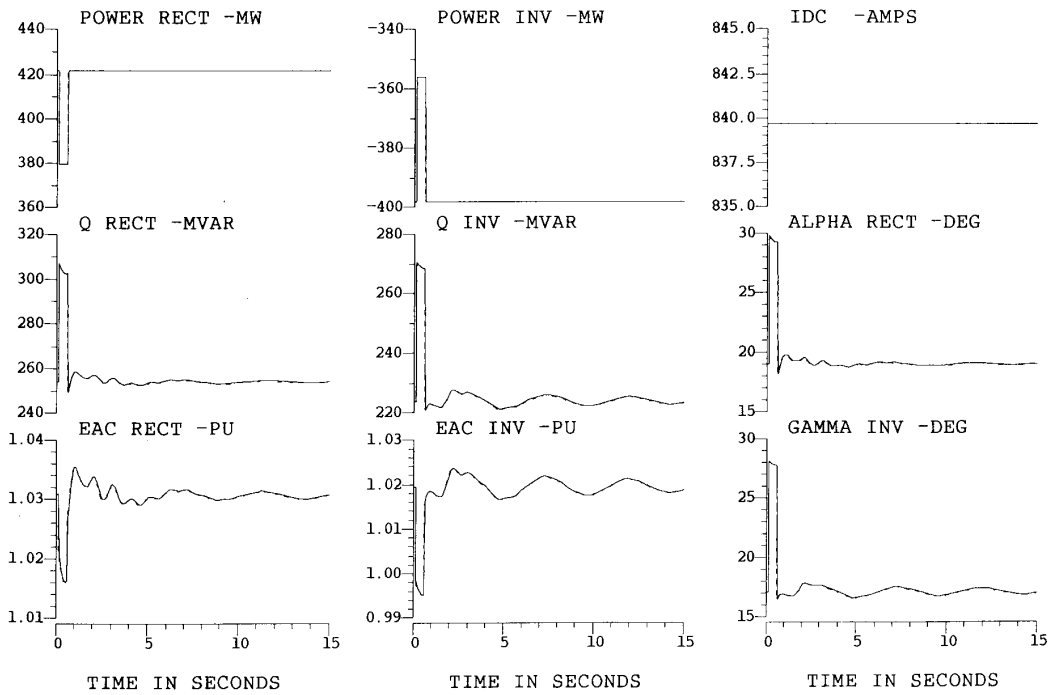


Figure 1b. Medium-scale MAPP model response for Square Butte dc voltage pulse. Square Butte system variables.

SNR implies sufficient input data points (153) and a high enough order of the linear prediction model. This generates sufficient accessory modes which produces consistency in the identification of "known" system modes from two ac frequencies at opposite ends of the dc system.

Prony parameters, the number of data points (N) and the order of the linear prediction model (n) are related, i.e. $n_{max} \leq N/2$. Reducing the number of data points from the 153 ($\Delta t = 0.087s, n = 69$) used for Table 1 results would decrease the signal-to-noise ratio and therefore the accuracy of the Prony fit to the time-domain plot (Figure 1a, DFREQ RECT). Halving the number of data points decreases the SNR by 6 db, 0.22 Hz mode damping from 5% to 1%, dominant modal frequencies by less than 1%. The Prony time step is typically larger than the time step of the digital model simulation, i.e. Table 1 results use 0.0876 s whereas the simulation integration time step uses 0.0042 s with a data output interval of 0.0292 s.

Table 1

Prony Solution for Rectifier Frequency

Mode	Damping	Frequency(Hz)	Rel. Wt.	Phase
3	0.0522104	0.2187290	0.3354653	93.3694447
4	0.1536905	0.6247455	1.0000000	74.3722889
5	0.1715984	0.7616728	0.1504237	146.5137449
6	0.5219796	0.7965686	0.6747275	-53.1662300
7	0.0706212	0.9843424	0.1424546	107.0915079
8	0.0596226	1.3162364	0.0378776	124.8723564
9	0.1306715	1.4662486	0.3424162	162.3473526
10	0.0861886	1.4767429	0.2223426	129.9128246
11	0.1356266	1.8227156	0.0867521	172.2609206
12	0.0546573	2.3820896	0.0578811	99.4133606

Prony results for inverter frequency are consistent with those in Table 1 for rectifier frequency. Accessory modes have low relative weight or high damping. Prony model results match input data with a SNR of 44 db. Plots of the two responses (not given) are indistinguishable. Table 2 gives excellent consistency of eigen- and Prony-analysis results for identification of interarea modal damping. Eigenanalysis uses all 450 states.

Table 2

Modal Damping (%) for the Medium-Scale Model
Interarea modes (Hz) for Eigen-and Prony-Analysis
(Bus Frequencies)

Freq.	Eigen Analysis	Prony	
		Rectifier	Inverter
.22	4.	5.	5.
.62	12.	15.	15.
.98	7.	7.	7.

CONTROL DESIGN MODEL IDENTIFICATION

Model identification can be accomplished using Prony analysis without and with parameter optimization. Parameter optimization minimizes response errors by adjusting pole/zero parameters for a fixed input structure [8]. Without parameter optimization, Prony analysis identifies poles and zeros associated with electromechanical modes based on controllability and observability (c/o). Differences of transfer functions between Prony and eigenanalysis cannot be reduced without parameter optimization.

Prony Analysis without Parameter Optimization

Model identification for control design involves the calculation of poles and zeros for "plant" transfer functions. Eigenanalysis permits calculation from state matrices directly. Retained modes are

based on controllability/observability using pole/zero cancellation [1]. Prony analysis calculates modes and residues to fit the reference signal.

Table 3 gives poles and zeros for a cascade structure for $\Delta f_r / \Delta E_d$. This is the ac/dc system response (Δf_r , rectifier frequency) to perturbations (ΔE_d) of the dc voltage reference of the dc line [7]. The interarea modes are in blocks 1, 2 and 5. Block 2 has only one simple zero to assure a physically realizable transfer function, i.e., the number of poles is greater than the number of zeros. All poles and zeros are in the left-half-plane.

Table 3

Poles and Zeros for Transfer Function $\Delta f_r / \Delta E_d$
Using Prony Analysis Alone

	Hertz	
1. Real Zeros	-0.38450476E-01	-0.24752542E+00
Complex Poles	-0.11435528E-01 + J*	0.21872896E+00
2. Single Zero	-0.12550836E+01	
Complex Poles	-0.97171926E-01 + J*	0.62474551E+00
3. Complex Zeros	-0.23930086E+00 + J*	0.33340639E+00
Complex Poles	-0.13266975E+00 + J*	0.76167284E+00
4. Complex Zeros	-0.11414007E+00 + J*	0.75418562E+00
Complex Poles	-0.48747130E+00 + J*	0.79656860E+00
5. Complex Zeros	-0.84460338E-01 + J*	0.92678885E+00
Complex Poles	-0.69689410E-01 + J*	0.98434236E+00
6. Complex Zeros	-0.90169474E-01 + J*	0.11078346E+01
Complex Poles	-0.78617274E-01 + J*	0.13162364E+01
7. Complex Zeros	-0.81042791E-01 + J*	0.13251788E+01
Complex Poles	-0.19325397E+00 + J*	0.14662486E+01
8. Complex Zeros	-0.15371985E+00 + J*	0.14838149E+01
Complex Poles	-0.12775374E+00 + J*	0.14767429E+01
9. Complex Zeros	-0.20549525E+00 + J*	0.17419921E+01
Complex Poles	-0.24951424E+00 + J*	0.18227155E+01
10. Complex Zeros	-0.16473561E+00 + J*	0.23089618E+01
Complex Poles	-0.13039345E+00 + J*	0.23820896E+01

Total Gain = 0.79858162E+00 19 Zeros 20 Poles

Tables 4a and b give eigenanalysis results. All poles and zeros are in the left-half-plane, as for the Prony Solution. Eigenvalues 6, 8 and 13 represent the three interarea modes. Some accessory modes are different for the two analysis methods. Prony analysis does not produce a simple pole at 2.00 rad/s (eigenvalue 12 in Table 4a).

Table 4a

Rectifier AC/DC System Poles for MAPP Mode
Model Using Eigenanalysis

	Real Part	Imag Part	Zeta	Freq (Hz)
1.	-2.512860D+01	+2.248067D-01	0.999960	3.577910D-02
3.	-2.474281D+01	0.000000D+00	1.000000	0.000000D+00
4.	-7.757016D-01	+9.010389D+00	0.085772	1.434048D+00
6.	-4.177420D-01	+6.185350D+00	0.067384	9.844290D-01
8.	-4.994577D-01	+4.010880D+00	0.123571	6.383514D-01
10.	-2.260215D+00	+2.155705D+00	0.723639	3.430910D-01
12.	-2.009330D+00	0.000000D+00	1.000000	0.000000D+00
13.	-5.820973D-02	+1.376159D+00	0.042261	2.190225D-01
15.	-4.995479D-01	+5.727221D-01	0.657323	9.115155D-02
17.	-1.999998D-01	1.000000D+00	1.000000	0.000000D+00
18.	-1.000000D-01	0.000000D+00	1.000000	0.000000D+00

Table 4b
Rectifier $\Delta f_r/\Delta E_d$ Transfer Function Zeros

	Real Part	Imag Part	Zeta	Freq (Hz)
1.	-1.100597D+00	+1.066985D+01	0.102606	1.698160D+00
3.	-5.445657D-01	+6.583050D+00	0.082441	1.047725D+00
5.	-6.910600D-01	+5.656957D+00	0.121260	9.003327D-01
7.	-2.260227D+00	+2.155713D+00	0.723640	3.430924D-01
9.	-1.106264D+00	+1.615385D+00	0.565032	2.570965D-01
11.	-7.829597D-01	0.000000D+00	1.000000	0.000000D+00
12.	-4.995472D-01	+5.727226D-01	0.657323	9.115163D-02
14.	-6.911610D-02	0.000000D+00	1.000000	0.000000D+00
15.	-2.646271D-12	+4.725443D-08	0.000056	7.520776D-09

Figure 2 gives transfer function Bode plots for the two methods. The features of the two responses are well matched over the range of electromechanical modes (0.2 to 2.0 Hz). Eigenanalysis has more peaking at the MAPP mode.

Table 5 gives a comparison of modal peaking, with peaking using Prony analysis about 6 db lower at 0.22 Hz. Other peaks are better matched as frequency increases. This may be due to the relatively short time-domain input (13.4 s).

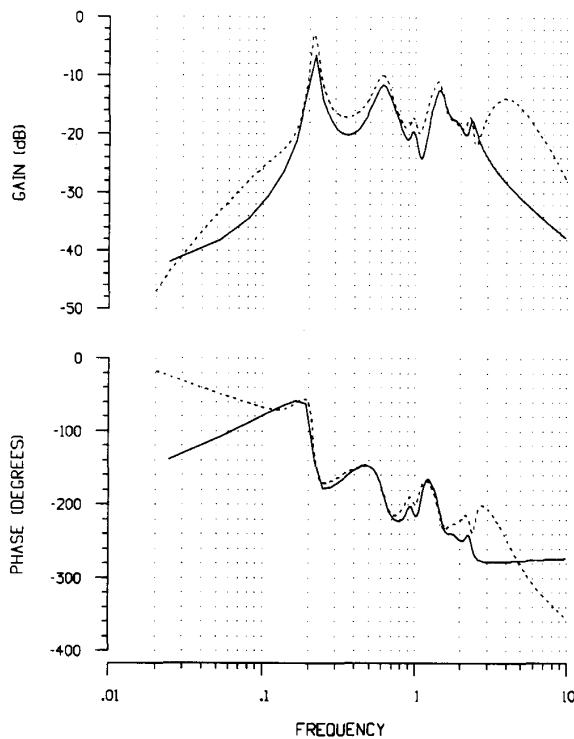


Figure 2. Transfer function ($\Delta f_r/\Delta E_d$) Bode plots, Prony analysis without BP filtering (—) Eigenanalysis (---).

Table 5
Resonant Peaking (db) for Rectifier and Inverter Transfer Functions ($\Delta f/\Delta E_d$) Using Eigen- and Prony-Analysis

Frequency	Rectifier		Inverter	
	Eigen-Analysis	Prony	Eigen-Analysis	Prony
.22	- 3.	- 9.	- 4.	-10.
.62	-10.	-12.	-12.	-15.
.98	-18.	-19.	- 6.	- 7.
1.30	—	—	-14.	-15.
1.48	-12.	-12.	—	—

Reviewing Figure 2 also shows that low frequency gain and phase do not match. This is due to high pass filtering of two stages: $s/(1+s)$ and $10s/(1+10s)$. Similarly, low-pass filtering is not properly represented in the Prony model due to lack of c/o. The lack of pass-band filtering in the Prony model can affect the gain and phase fidelity at low and high frequencies. The effects of band-pass filtering can be added manually to the Prony model after poles and zeros due to electromechanical modes have been identified.

Prony Analysis with Parameter Optimization

High-pass and low-pass filters were added to the Prony solution. The high-pass filter parameters were adjusted by the parameter optimization routine with gain matching only. The resulting gain and phase (Figure 3) match the reference in the low frequency region (< 0.1 Hz) very well.

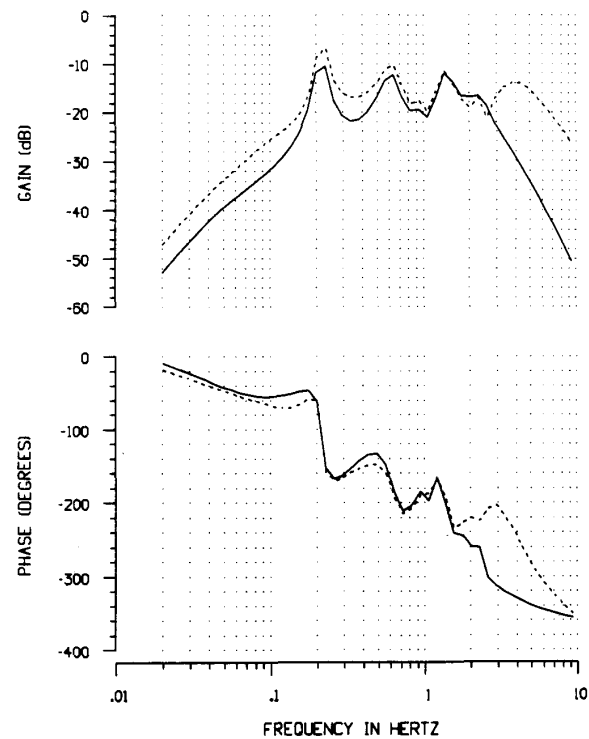


Figure 3. Transfer function ($\Delta f_r/\Delta E_d$) gain and phase plots with variable high-pass and low-pass filters. Prony (—), eigenanalysis (---).

Low-pass filter parameters were optimized (Table 6). Now the phase error trends toward zero at high frequencies. A right-half-plane pair of zeros is introduced at 0.0037 Hz, Block 11, by the parameter optimization routine. Since this corresponds to -360° over left-half-plane complex zeros, the net effect is zero. A simple right-half-plane pole with 17.2 ms time constant is introduced to produce 180° of phase advance over a left-half-plane pole. The remaining gain and phase error above 2 Hz is due to the difference in structure for the parameter optimization routine input compared to the reference frequency response input, which has two complex lead/lags (torsional notch filters).

Table 6
Poles and Zeros for Transfer Function $\Delta f_r/\Delta E_d$
With Variable High Pass and Low Pass Filters

	Hertz
1. Complex Zeros	-0.17951825E+00 + J*0.83772548E-01
Complex Poles	-0.11435528E-01 + J*0.21872896E+00
2. Single Zeros	-0.46208095E+00
Complex Poles	-0.97171926E-01 + J*0.62474551E+00
3. Complex Zeros	-0.21638250E+00 + J*0.35027111E+00
Complex Poles	-0.13266975E+00 + J*0.76167284E+00
4. Complex Zeros	-0.86755937E-01 + J*0.75827669E+00
Complex Poles	-0.48747130E+00 + J*0.79656860E+00
5. Complex Zeros	-0.76854413E-01 + J*0.92759105E+00
Complex Poles	-0.69689410E-01 + J*0.98434236E+00
6. Complex Zeros	-0.95817413E-01 + J*0.11063721E+01
Complex Poles	-0.78617274E-01 + J*0.13162364E+01
7. Complex Zeros	-0.93835143E-01 + J*0.13250362E+01
Complex Poles	-0.19325397E+00 + J*0.14662486E+01
8. Complex Zeros	-0.11823443E+00 + J*0.14872728E+01
Complex Poles	-0.12775374E+00 + J*0.14767429E+01
9. Complex Zeros	-0.16220320E+00 + J*0.17467179E+01
Complex Poles	-0.24954134E+00 + J*0.18227155E+01
10. Complex Zeros	-0.16567381E+00 + J*0.23091536E+01
Complex Poles	-0.13039345E+00 + J*0.23820896E+01
11. Complex Zeros	0.23116623E-02 + J*0.37057572E-02
Complex Poles	-0.54862111E-01 + J*0.23358286E-01
12. Complex Poles	-0.39779257E+01 + J*0.87242321E-01
13. Single Pole	0.92654687E

Total Gain = 0.60281830E + 05 21 Zeros 25 Poles

The above parameter optimization results are a few of the many variations that can be achieved by variations of structures and fixed versus variable parameters. Right-half-plane poles and zeros produced by the parameter optimization routine are related to phase fit and, therefore, phase fit should be delayed if not avoided completely. Gain and phase fit for the Prony method could have been improved above 1.5 Hz by including two complex biquad blocks for the torsional filters at 11.5 Hz that are included in the eigenanalysis.

CONCLUSIONS AND RECOMMENDATIONS

Prony analysis and eigenanalysis are complementary methods. This paper has started with a typical stability model and shown that both can produce similar results in the determination of modal parameters and the construction of controller design models. However, like all identification procedures, Prony analysis demands care in the choice of processing parameters and should be used in combination with other methods. The example presented here provides guidance in this, and is a progress report in the continuing

development of a very promising tool.

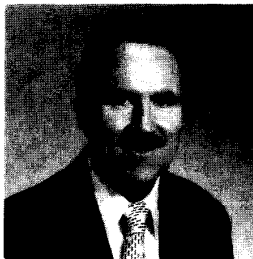
Each situation differs and the parameters given may be used as a starting point only. There are other methods [14] which like Prony analysis, also do not require a full state matrix for digital model analysis. However, they [14] would not be useable for field measurement analysis.

ACKNOWLEDGMENTS

Since the applications data originated from the MAPP model for EPRI RP1426-4 (HVDC Modulation), which was provided by Minnesota Power, we would like to acknowledge the contributions of Messrs. D.L. Carlson, L.P. Crane, S.R. Norr, and G. Sweezy, Minnesota Power.

REFERENCES

- [1] C.E. Grund, R.J. O'Keefe, J.J. Paserba, D.L. Carlson, S.R. Norr, "Development of Low-Order Control Design Models from Standard Stability Models," Eigenanalysis and Frequency Domain Methods for System Dynamic Performance, IEEE Publication 90TH0292-3-PWR, 1989.
- [2] E.V. Larsen, W.W. Price, "MANSTAB/POSSIM Power System Dynamic Analysis Programs - A New Approach Combining Nonlinear Simulations and Linearized State-Space/Frequency Domain Capabilities," IEEE PICA Proceedings, 1977.
- [3] J.F. Hauer, C.J. Demeure, and L.L. Scharf, "Initial Results in Prony Analysis of Power System Response Signals," IEEE Trans. Power Systems, pp. 80-89, February 1990.
- [4] J.F. Hauer, "Application of Prony Analysis to the Determination of Model Content and Equivalent Models for Measured Power System Response," IEEE Trans. Power Systems, pp. 1062-1068, August 1991.
- [5] J.F. Hauer, "Reactive Power Control as a Means for Enhanced Interarea Damping in the Western U.S. Power System - a Frequency-Domain Perspective Considering Robustness Needs," Application of Static Var Systems for System Dynamic Performance, IEEE special publication 87TH0187-5-PWR, 1987.
- [6] C.E. Grund, S.E. Wright, "HVDC Modulation for Flexible AC/DC Transmission Systems," presented at CIGRE SC-14 Colloquium, Rio de Janeiro, August 1, 1989.
- [7] C.E. Grund, H.W. Mosteller, D.L. Carlson, L.P. Crane, S.E. Wright, "Application of Advanced HVDC Modulation Techniques to Large-Scale Power Systems," Presented at the CIGRE Conference on AC/DC Transmission Interactions, Boston, September 1987.
- [8] J.F. Hauer, "Power System Identification by Fitting Structured Models to Measured Frequency Response," IEEE Transactions on Power Apparatus and Systems, Vol. PAS-101, No. 4, pp. 915-923, April 1982.
- [9] J.F. Hauer, and F. Vakili, "An Oscillation Trigger for Power System Monitoring," IEEE Trans. Power Systems, pp. 74-79, February 1990.
- [10] D.J. Trudnowski, J.R. Smith, T.A. Short, and D.A. Pierre, "An Application of Prony Methods in PSS Design for Multimachine Systems," IEEE Trans. Power Systems, pp. 118-126, February 1991.
- [11] J.F. Hauer, "Robust Damping Controls for Large Power Systems," IEEE Control Systems Magazine, January 1989.
- [12] J.F. Hauer, "BPA Experience in the Direct Measurement of Power System Dynamics," IEEE/PES 1991 Winter Meeting Symposium of Inter-Area Oscillations, New York, February 6, 1991.
- [13] C. Chen, "Linear Systems Theory and Design," Holt, Rinehart and Winston, New York, 1984.
- [14] P. Kunder, G.J. Rogers, D.Y. Wong, L. Wang, and M.G. Lauby, "A Comprehensive Computer Program Package for Small Signal Stability Analysis of Power Systems," IEEE Trans. Power Systems, pp. 1076-1083, November 1990.



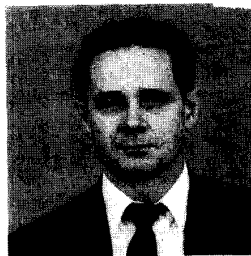
Carl E. Grund (Senior Member) is a project manager in the Power Systems Engineering Department of GE Industrial and Power Systems, Schenectady, N.Y. He received the B.S.E.E. degree from San Jose State University and the M.S.E.E. in Systems Science and an Engineer Degree in System Engineering from the Polytechnic Institute of New York. He completed the GE Advanced Engineering Course. He was project engineer on various HVDC Dynamic Performance Studies. Present research and development involvement is in the application of advanced control design methodology to hybrid ac/dc systems. Previous responsibility was in control design of variable speed ac drives. Within the IEEE, he has been the Chairman of the Dynamic Performance and Modeling Working Group within the Transmission and Distribution Committee. He has authored numerous articles in the areas of control, HVDC transmission and dynamic performance analysis of large scale power systems. He is a member of Tau Beta Pi and Phi Kappa Phi.



John Paserba (S'84, M'89) received his BEE from Gannon University, Erie, Pennsylvania in 1987 and his ME in Electric Power Engineering from Rensselaer Polytechnic Institute, Troy, New York in 1988.

Mr. Paserba joined GE in Schenectady, New York in 1988 as an Application Engineer. In that position, he is involved with the analysis of power system dynamics using both time- and frequency-domain techniques, and the study of controls to improve power system dynamic behavior.

Mr. Paserba is a member of IEEE Power Engineering Society and the IEEE-PES Working Group on System Oscillations.



John F. Hauer (S'59-F'90) was born in Washington State in 1936. He received the B.S. degree (summa) at Gonzaga University in 1961, and the Ph.D. degree at the University of Washington as a National Science Foundation Graduate Trainee in 1968. Both were in electrical engineering.

In 1961 and 1962 he was with GE, working in the area of nuclear reactor controls while enrolled in the Advanced Engineering Training Program. In 1963 and 1964 he developed spacecraft navigation and guidance methods at the Boeing Company, for use in lunar mapping. His subsequent doctoral research addressed methods for designing safety factors into thrusting trajectories for interplanetary flight. From 1968 to 1975 he was a member of the Computing Science faculty at the University of Alberta. His activities there centered upon constrained optimization of dynamic systems. Since 1975 he has been with the Bonneville Power Administration. His work there deals with the identification, analysis and control of power system dynamics.

Dr. Hauer is a member of the IEEE Power Engineering and Control Systems societies.



Stig L. Nilsson (F'88) is a Senior Program Manager, Transmission Substations Program in the Electrical Systems Division, at the Electric Power Research Institute (EPRI) in Palo Alto, California. Before joining EPRI in 1975, Nilsson worked for three years at The Boeing Company, assigned to the Boeing Electronic Utility Instrumentation and Control Department in the Portland, Oregon office. He spent the last six months with the company in the Computer Services Division as a Program Manager. Between 1962 and 1972, Nilsson worked for ASEA Sweden, at first involved with simulation of HVDC systems. In 1963, he was assigned to the ASEA Konti-Scan HVDC project as Control Engineer, and in 1967 he was assigned to the ASEA-GE joint venture project for the Pacific HVDC Intertie Project.

Nilsson holds an E.E. degree, obtained at HTL, Malmoe, Sweden in 1960 and an MBA from Santa Clara University in 1985. He is a Fellow of IEEE, chairman of a working group of the Power Systems Relaying Committee, chairman of the DC Transmission Subcommittee in the Transmission and Distribution Committee and a member of CIGRE and CIGRE working groups. He is also the author of numerous papers on HVDC and digital control and protection of substations. He received the Prize Paper Award from IEEE Power Engineering Society in 1987 and was elected as a Fellow by the IEEE Board of Directors in 1988.

Discussion

J. R. Smith (Montana State University, Bozeman, MT): Congratulations to the authors for an interesting comparison of transfer functions using state space linearization versus time series analysis. Our experience with early versions of the Prony algorithm indicated that it can be very difficult to obtain accurate transfer function fits in dealing with HVDC systems. The authors' attempts obviously have been fairly successful. In dealing with Prony analysis we have noted that the shape of the input pulse can occasionally have a significant impact on the accuracy of the Prony transfer function parameters. It is interesting to note that in Fig. 2 of the paper the frequency response of the two models begin to diverge around 2 Hz. If the input pulse which was used to generate the data was a square pulse 1/2 second in duration (as in the first example) then the energy spectrum of the input will be very low in the frequency range of 2 Hz. This is due to the Fourier Transform of the square pulse being the sine function which goes to zero at intervals of $1/T$ Hz where T is the width of the pulse. This will make it very difficult to accurately identify modal parameters at frequencies near $1/T$ Hz due to a relative lack of excitation. In our experiments we have found best results in power system electromechanical cases if we restrict the pulse length to be less than 0.2 seconds and 0.1 seconds is most commonly used. It could be possible that this phenomena is why the Prony algorithm did not accurately identify the dynamic phenomena in the 2 Hz range reported by the state space eigenanalysis method.

A second point concerns the low frequency behavior seen in the frequency response plots of Fig. 2. The Prony case has increasing gain and increasing phase at low frequencies which is consistent with left half plane zeros at low frequencies (real zeros of mode 1 in Table 3). The state space eigenanalysis curve of Fig. 2 shows increasing gain with decreasing phase which suggests a characteristic predominated by right half plane zeros.

Table 4b however shows no right half plane zeros resulting from the state space method. It may be worth checking on the possibility that either the real zeros listed in Table 4b (#11 and #14) have the wrong sign or else the frequency response plot may be in error. The fact that right half plane zeros were added to the Prony model to obtain the improved fit in Fig. 3 suggests that the state space method zeros listed in Table 4b must have some sign errors.

C. E. Grund, J. J. Paserba, J. F. Hauer, S. J. Balsler, and S. Nilsson: The authors appreciate the encouraging remarks of Dr. Smith and the comments and the contributions to the paper.

The authors agree completely with the recommendation to use a shorter pulse for pushing the input null to a higher frequency. The input pulse width of 0.5 S produced a null at 2.0 Hz and, therefore, for greater accuracy of the Prony method a shorter pulse width would be desirable.

The lack of a better fit above 1.6 Hz can be attributed to the constraint on the structure of the Prony model. It was constrained to simple poles to match phase in the limited frequency range of the control design model whereas the eigenanalysis (EA) model had complex poles and zeros of a torsional filter at 11.5 Hz.

Regarding the second point, some additional discussion of the EA results should clarify the issue. The EA results are a reduced order equivalent of a 450 state model for control design with control effectiveness over a frequency range of 0.2 to 1.6 Hz, the range of important electromechanical oscillations surrounding the Square Butte DC System. Poles and zeros with effects outside of the designated frequency range were eliminated, i.e. too low frequency would produce -180 degrees phase shift in the frequency range of interest and, therefore, only the phase (negation) was represented in the control design model.